Modeling and Experimental Studies of Emulsion Copolymerization Systems. II. Styrenics

ENRIQUE SALDÍVAR,[1] ODAIR ARAUJO,[2] REINALDO GIUDICI,[3] CARLOS LÓPEZ-BARRÓN[1]

[1] CID-GIRSA Corporativo S. A. de C. V., Av Sauces 87 Mza.6 Lerma, México

[2] Rhodia, Campinas S. P. Brasil

[3] Departamento de Engenharia Química, Universidade de São Paulo, Brasil

Received 27 December 1999; accepted 3 May 2000

ABSTRACT: Using a model previously published, predictions for evolution of conversion and average particle diameter in batch experiments are compared against experimental data for four emulsion copolymerizations of styrene with the following monomers: (1) methyl methacrylate, (2) butyl acrylate, (3) butadiene, and (4) acrylic acid. For each copolymerization system the experiments covered simultaneous variations in five variables: initiator and surfactant concentrations, water to monomer ratio, monomer composition, and temperature. It is shown that after data fitting for unknown or uncertain parameters, the model is capable of explaining quantitatively the experimental observations for conversion evolution and only qualitatively the particle size evolution data. This points out to the possible contribution of particle nucleation mechanisms other than the micellar one, which is the only mechanism included in the model. Some of the adjustable parameter values were found to depend on the copolymer composition. The only case in which the model does not perform well is in the prediction of the effect of initiator concentration on the copolymerization rate for butadiene-rich formulations. It is also found that the model predictions are very sensitive to the value of the diffusion coefficients of monomeric radicals in the copolymer particle, which are not readily available in the literature. It is concluded that it is important to independently measure these parameters in order to enhance the predictive power of models. It is also concluded that the model can be useful for practical applications. © 2001 John Wiley & Sons, Inc. J Appl Polym Sci 79: 2380–2397, 2001

Key words: emulsion copolymerization; mathematical modeling

INTRODUCTION

In the first part of this series of papers experimental results for a number of copolymer systems produced by emulsion polymerization were presented and discussed. In this second part more detailed studies, which include simulations, are presented for the styrenic copolymerization systems included in the first part of the series. Experimental data and simulations for the systems methyl-methacrylate/styrene, butyl acrylate/styrene, butadiene/styrene, and acrylic acid/styrene are presented and contrasted.

Styrene polymers and copolymers are some of the most studied systems due to their industrial and scientific importance. Industrially, a second monomer is copolymerized with styrene in order

Correspondence to: Enrique Saldívar (esaldiva@mail.girsa.com.mx).

Journal of Applied Polymer Science, Vol. 79, 2380–2397 (2001)

to enhance the physical properties of polystyrene, still preserving its good processability and reasonable cost of production. From the scientific standpoint, emulsion homo- and copolymerization of styrene have long been used as models for the study of theories of emulsion polymerization. In spite of this, very few studies have been published in which the copolymerization of styrene with several monomers is considered and contrasted; most of the studies of copolymerization of styrene with other monomers have concentrated on only one comonomer.

To date deterministic modeling of free-radical and emulsion copolymerization has been tackled in two ways:

1. An empirically oriented one in which most of the parameter values of the system are fitted to data, even when some of the parameters could be measured by independent experiments. An example of this is the work of García-Rubio et al.[1] This approach tends to yield good fitting of the experimental data and the resulting model can be used for engineering purposes as a tool for interpolation.
2. A fundamentally oriented approach in which most of the parameter values are taken from independent sources. In this case data fitting is kept to a minimum and parameter values that come from independent experiments are taken from the literature or are estimated *a priori*, but only qualitative behavior and trends are predicted (see, for example, ref. 2). Through this approach the general plausibility of the model can be evaluated, but a quantitative assesment of the practical applicability of the model is not possible.

A third approach could be considered as an intermediate one and is the one adopted in this work. In this approach all parameters for which reliable values are available are taken from the literature. On the other hand, unknown or uncertain parameters are fitted to experimental data restricting the adjusted parameter values to lie between physically reasonable limits. Through this approach both the theoretical plausibility of the model as well as its practical applicability can be assessed. Forcing the predictive capability of the model to an extreme may help detect weak aspects of the model. This approach is especially useful in modeling of systems that exhibit high complexity as in the case of emulsion copolymerization. Some authors have recently even questioned the possibility of modeling this kind of systems (van Herk and German[3]).

In this work the experimental data of Araujo et al.[4] for four emulsion copolymerizations of styrenic systems are discussed with the help of a general mathematical model for emulsion copolymerization presented elsewhere.[5] Two goals are pursued in this paper: (1) to gain insight about the mechanisms governing emulsion copolymerization reaction rate, especifically for styrenic systems; and(2) to assess to what extent the present understanding of emulsion copolymerization, cast in the form of a general mathematical model, is quantitative and readily applicable, and in which specific areas of emulsion copolymerization theory, as seen by the authors, there is a need for more in-depth research.

In the next section a brief review of previous work published in the literature on styrene emulsion copolymerization is given. In the experimental section of this study the experiments perfomed on the methyl-methacrylate/styrene, butyl acrylate/styrene, butadiene/styrene, and acrylic acid/styrene systems are presented. A summary of the mathematical model proposed earlier by Saldívar et al.[5] is also discussed. Next, styrenic systems are simulated with the mathematical model described in the previous section and the predictions of the mathematical model are discussed and contrasted with the experimental data.

PREVIOUS WORK

Methyl methacrylate/styrene (MMA/S) emulsion copolymerization has been studied by several authors. Ballard et al.[6] used this system to experimentally validate the pseudo-homopolymer approach (also known as method of apparent or pseudo-kinetic rate constants) for emulsion copolymerization. Goldwasser and Rudin[7] did experimental work in order to estimate the rate coefficients for transfer to monomer in this system. Nomura et al.[8] studied the effects of initiator concentration and monomer composition on polymerization rate and number of particles; they also found that desorption of MMA radicals from particles may significantly decrease the rate of polymerization. Chen and Wu[9] extended the Ballard et al. model to describe the distribution of particle sizes for the system MMA/S. Nomura et al.[10] presented an experimental and modeling work for

the unseeded emulsion copolymerization of MMA/S. They found that the final number of particles increases weakly with initiator concentration and with MMA fraction in the monomer mixture, and depends more strongly on the emulsifier concentration in excess of its critical micellar concentration (CMC). In another work Nomura et al.[11] studied in more detailed the nucleation step and concluded that coagulation can be neglected.

Forcada and Asua[12,13] studied the effect of initial monomer composition over the rate of copolymerization, number of particles and final molecular weight. They also wrote a mathematical model to explain their data and fitted some of the parameters of the model to get agreement with the experimental data. Notably they fitted entry rate coefficients to fit copolymerization rate data and transfer to monomer rate coefficients to fit the molecular weight data. Noel et al.[14] performed a sensitivity analysis of an emulsion copolymerization mathematical model to show that monomer solubility differences for this system will be important only at very low monomer to water ratios. Saldívar and Ray[5] also used a mathematical model to explain their experimental data showing combined effects of initiator and emulsifier concentration on copolymerization rate and evolution of particle size. These authors also fitted entry rate coefficients and emulsifier adsorption parameters in order to fit their model predictions to data.

Butyl acrylate/styrene (BuA/S) emulsion copolymerization was studied by Cruz et al.[15] and Cruz-Rivera et al.,[16] Guillot ,[17] Canegallo et al.,[18] Gugliotta et al.,[19] and López de Arbina et al.[20] In order to study the effect of structure of the polymer on its properties, Cruz-Rivera et al. prepared model copolymers of BuA/S by several processes: corrected batch, core-shell, and multistep polymerizations. Their main goal was to investigate the filming properties of latexes prepared with different processes. From a more fundamental point of view, they developed simulation models that explain the evolution of copolymer composition and T_g. They also show simulations for global conversion vs time, but these were obtained feeding the model with experimental data of rate of polymerization vs conversion, so these simulations are rather a tool for calculation of intermediate values in kinetic expressions (k_p, $\tilde{n}$) than a predictive tool.

Guillot[17] studied the system BuA/S and found that the global coefficient for the rate of propagation can be predicted by the classical theory of free radical copolymerization. He also found that in BuA-rich formulations, this monomer tends to react toward high conversions and proposed a core-shell particle morphology to explain this fact. Canegallo et al.[18] compared batch and semicontinuous emulsion copolymerizations for the same system. They developed a strategy for the control of composition feeding styrene in order to maintain a homogeneous composition.

Gugliotta et al.[19] studied the modeling of monomer partitioning in several emulsion copolymerization systems. They found that in systems with high solid contents (around 55%) or medium solid contents (30%), but with seeds exceeding 10%, partitioning results are independent of the partitioning model used. The same was found not true for lower solid contents.

López de Arbina et al.[20] used calorimetric measurements to study the kinetics of seeded emulsion copolymerization of BuA/S with 60/40 initial composition. They varied the diameter of the seed, number of seed particles, and initial initiator concentration. A mathematical model was used to fit experimental data of conversion vs time using the entry and desorption coefficients as adjustable parameters.

Several researchers have experimentally investigated the emulsion copolymerization of butadiene/styrene (B/S). Mitchel and Williams[21] discussed the curves conversion–time for the systems B/S 50/50, 40/60, 30/70, 20/80, and 10/90 at 50°C. Carr et al.[22,23] studied the effect of emulsifier type on the polymerization at 50°C for a ratio B/S 75/25. Burnett et al.[24–26] studied the time evolution of copolymer composition, reaction rate and crosslinking phenomena at 5, 15, and 25°C.

Hamielec and MacGregor,[27] Broadhead et al.,[28] Gugliotta et al.,[19] and Sayer et al.[29] developed mathematical models of several levels of detail for the emulsion copolymerization of butadiene/styrene. Their emphasis is on applications for the industrial production of SBR, synthetic rubber for use in tires.

The kinetics of emulsion polymerization of butadiene and of butadiene/styrene is complex and is not well explained by traditional theories of emulsion polymerization. It has been found that the rate of emulsion polymerization of butadiene[30] and that of copolymerization of butadiene/styrene[31] is almost independent of initiator concentration. Weerts et al.[30] also mention that values reported in the literature for the propagation rate coefficient k_p of butadiene, might be in gross error due to mass transfer effects interferring

with its estimation. These authors also suggest a low value for $\tilde{n}$ (<0.5), probably due to desorption of radicals, in spite of the low water solubility of butadiene. Bachman et al.[32] found a value for ñ that depends on the particle size; they modeled this effect by distinguishing between mobile radicals at the particle surface and immobile radicals inside the particles.

Butadiene/styrene copolymerization produces a material that can present some extent of gel due to the presence of a second double bond in the polymerized units of butadiene, which can undergo crosslinking reactions. This aspect has only recently been studied through mathematical modeling due to the technical difficulties that it poses, especially during and after the transition of the pre-gel to the post-gel regime. Tobita and Hamielec[33] presented a kinetic-based model for the crosslinking reactions and gel formation . Charmot and Guillot[34] experimentally studied the gel formation in the emulsion copolymerization of styrene/butadiene and compared their data with the results predicted by a mathematical model of the phenomenon based on statistical principles.

Although much effort has been put in the last two decades on the mathematical modeling of the kinetics of copolymerization and gel formation for the butadiene/styrene system, the rubber industry still bases its quality control on measurements such as the Mooney viscosity, which is known to depend on the molecular weight of the copolymer and the extent of crosslinking, but there is still no clear way to relate the practical measurements with the more fundamental parameters.

Acrylic acid is a totally water soluble monomer so, during emulsion polymerization, most of the polyacrylic acid resides in the aqueous– particle interphase. In this way the presence of acrylic acid acts as an stabilizer of the emulsion system. Also, this monomer increases the rate of homogeneous nucleation.

Ceska[35] studied the use of acrylic acid in soapless emulsion copolymerization with styrene at 70°C. It was found that the acrylic acid increases the rate of polymerization and the number of particles. Guillot[17] studied the variation of the propagation rate coefficient and the reactivity ratios in systems with carboxylic monomers. He found that the propagation rate depends on the ratio of ionized/nonionized carboxylic acid and that this ratio depends on the pH of the emulsion system.

Table I Experimental Design: Methyl Methacrylate/Styrene System[a]

Run	Temperature	Styrene Level	[*I*]	[*E*]	*M*/*W*
1	−	−	−	+	+
2	+	−	−	−	−
3	−	+	−	−	+
4	+	+	−	+	−
5	−	−	+	+	−
6	+	−	+	−	+
8	+	+	+	+	+
10	−	−	−	−	−
11	+	−	+	+	+
12	−	+	−	−	−

[a] Temperature [+] = 70°C, [−] = 60°C; % MMA/% S: [+] = 30/70, [−] = 70/30; [*I*]: [+] = 0.004 mol/L-aq, [−] = 0.002 mol/L-aq; [*E*]: [+] = 0.028 mol/L-aq, [−] = 0.014 mol/L-aq; monomer to water ratio (wt): [+] = 0.55, [−] = 0.34.

EXPERIMENTAL

The emulsion polymerizations were performed in a reaction system consisting of a 2.4 l.TDH Mfg., Inc., reactor equiped with a magnetic stirrer having a 4-blade turbine working at 254 rpm. The temperature control was achieved by using a water bath with a centrifugal circulation pump and a CN76000 Omega controller. The temperature was controlled within ±0.5°C of the setpoint. The experimental procedure followed during the polymerizations and the complete experimental design are given in ref. 4. Here, only those parts of the experimental design that were simulated and analyzed with the mathematical model are shown in Tables I–IV. The run numbers correspond to the experiments discussed in ref. 4 and 36.

THEORETICAL FRAMEWORK

In Appendix A the kinetic scheme for a general emulsion copolymerization is presented according to Saldívar et al.[5] The mathematical solution of the model implemented in the POLYRED software package was used. In this implementation the PDE representing the particle size distribution (PSD) is discretized using orthogonal collocation on finite elements with moving boundaries.[37] The resulting set of ordinary differential equations (ODEs), together with the differential-algebraic equation (DAE) system representing the material balances for species and the thermody-

Table II Experimental Design: Butyl Acrylate/ Styrene System

Run	Temperature	Styrene Level	[*I*]	[*E*]	*M*/*W*
1	−	+	+	+	−
5	−	−	−	+	−
6	−	+	−	+	−
7	−	+	−	−	+
12	−	+	−	−	−
13	−	−	−	−	−

[a] Temperature: [+] = 70°C, [−] = 60°C; % BuA/% S: [+] = 30/70, [−] = 70/30; [*I*]: [+] = 0.004 mol/L-aq, [−] = 0.002 mol/L-aq; [*E*]: [+] = 0.028 mol/L-aq, [−] = 0.014 mol/L-aq; monomer to water ratio (wt): [+] = 0.55, [−] = 0.34.

namic equilibrium equations for monomer partitioning, are solved using the software DDASSL.[38]

RESULTS AND DISCUSSION

For each one of the copolymerization systems those parameters of the model not available in the literature were adjusted using conversion–time and particle size–conversion data. The parameters used for fitting the data were the CMC of the emulsifier , the Γ_∞ and b_S parameters of the adsorption isotherm for the emulsifier , the entry rate coefficients k_{mmi} and k_{mmR} and an effective diffusion coefficient ($D_{\text{eff},i}$) for desorption of monomeric radicals from the particle [eqs. (1) and (5)–(8)].

Fitted parameters can be grouped in two categories: (1) those measurable by independent experiments like $D_{\text{eff},i}$,CMC, a_{em}, Γ_∞, and b_S (although their values may be significantly affected by the presence of monomers); and (2) those strongly dependent on the specific model used, like k_{mmi} and k_{mmR} and gel effect parameters. In this work parameters used for fitting the data were chosen because either (1) there are no independent measurements for these quantities, (2) the values of the parameters significantly depend on the specific components present in the polymerization recipe, or (3) parameters are model dependent.

Table III Experimental Design: Butadiene/Styrene System

Run	Temperature	Styrene Level	[*I*]	[*E*]	*M*/*W*
1	−	+	−	−	−
2	−	−	−	−	−
5	−	+	+	+	−
6	−	−	+	−	−
14	−	−	+	+	−
15	−	+	−	+	−
16	+	+	−	−	−
17	+	−	−	−	−
18	+	−	−	+	−

[a] Temperature: [+] = 80°C, [−] = 70°C; % B/% S: [+] = 30/70, [−] = 70/30; [*I*]: [+] = 0.004 mol/L-aq, [−] = 0.002 mol/L-aq; [*E*]: [+] = 0.028 mol/L-aq, [−] = 0.014 mol/L-aq; monomer to water ratio (wt): [−] = 0.34.

Table IV Experimental Design: Acrylic Acid/ Styrene System

Run	Temperature	Styrene Level	[*I*]	[*E*]	*M*/*W*
7	−	+	+	−	−
9	−	+	−	−	−

[a] Temperature: [−] = 60°C; % AA/% S: [+] = 5/95; [*I*]: [+] = 0.004 mol/L-aq, [−] = 0.002 mol/L-aq; [*E*]: [−] = 0.014 mol/L-aq; monomer to water ratio: [−] = 0.34.

With respect to the area a_{em} of a micelle covered by a surfactant molecule , Morbidelli et al.[39] point out that this parameter depends on the ionic strength of the solution and that it is erroneous to assume that $a_{em} = a_{ep}$, where a_{ep} is the area of a polymer particle covered by a surfactant molecule (its experimental value is generally unavailable for specific systems). Also, the adsorption of surfactant to particles is reported by the same authors to be well represented by a Langmuir isotherm, but the parameters for specific systems are not readily available since they have to be obtained experimentally for each system. Entry rate coefficients k_{mmi} and k_{mmR} were also fitted as they strongly depend on the model employed and only a few attempts have been made in order to independently measure these quantities.[40] As for gel effect, this phenomenon is qualitatively well understood, but available models still lack predictive power, especially for copolymerization systems. The gel effect equations used were those given in Table V in which subindexes 1 and 2 refer to a comonomer and styrene, respectively. The form of the individual gel effect correlations were taken from Schmidt and Ray[41] for the comonomer and from Morbidelli et al.[39] for styrene. The form of general correlations was taken from ref. 5. Values for two independent parameters A_5 and A_7 (the value of a third one A_6, is given by continuity constraints) were fitted for

Table V Gel Effect Correlations

Styrene (2)
$g_{p2} = 1$
$g_{t2} = \exp(S_1x + S_2x^2 + S_3x^3)$
Comonomer (1)
$V_{fi} = A_0 + A_1(T_K - A_2)$
$V_{fpi} = A_0 + A_3(T_K - A_4)$
$V_{fi} = \phi_{p1}V_{f1} + \phi_{p2}V_{f2} + \phi_{pp}\ \Sigma_{j=1}^{c}$
$\Phi_{\mathrm{pi}}V_{\mathrm{fpi}}$
$g_{p1} = 1$ for $V_f > A_5$
$g_{p1} = A_6\exp(A_7V_f)$ for $V_f < A_5$
$V_{fc} = A_8 - A_9T_c$
$g_{t1} = A_{10}\exp(A_{11}V_f - A_{12}T_c)$ for $V_f > V_{fc}$
$g_{t1} = A_{13}\exp(A_{14}V_f)$
General
$g_p = g_{p1}^{\Phi_{p1}}g_{p2}^{\Phi_{p2}}$
$g_t = (g_{t1}g_{t2})^{1/2}$
$k_{tii} = g_tk_{t0ii}$
$k_{pii} = g_pk_{p0ii}$
$k_{t12} = k_{t21} = \phi(k_{t11}k_{t22})^{1/2}$
$k_{tr12} = k_{tr21} = \phi(k_{tr11}k_{tr22})^{1/2}$
$k_{pij} = k_{pii}/r_{ij}$

[a] x = total conversion; T_K = temperature in °K; T_c = temperature in °C; V_{fi} = free volume of component i; V_{fpi} = free volume of homopolymer i, ϕ_{pi} = volume fraction of component i in particles; Φ_{pi} = mass fraction of component i in copolymer; r_i = copolymer reactivity ratio for monomer i.

the glass region (diffusion-limited propagation) of the comonomer gel effect correlation.

With respect to the desorption coefficient d, the mathematical model used, as well as other existing models, proposes a mixing rule for the calculation of the pseudo-homopolymer desorption coefficient [see Eqs. (5)–(8) in Appendix A], which ultimately depends on the values of the diffusion coefficients of the monomeric radicals of each type in water and in the polymeric media (D_{wi} and $D_{pi,}$ respectively). Furthermore, due to the way in which these coefficients appear in the equations [see eq. (8)] it is virtually impossible to obtain independent estimates for these parameters using a global model as the one employed in this work. Instead, an effective value $D_{\mathrm{eff},i}$ for the diffusion of type i radicals in the particles was estimated, defined as

$$\frac{D_{\mathrm{eff},i}}{3} = \frac{D_{wi}D_{pi}}{m_{di}D_{pi} + 2D_{wi}} \qquad (1)$$

During the first fitting trials it was assumed that the values $D_{\mathrm{eff},i}$ could be taken, as a first guess, as those of the type i monomeric radical in its own homopolymer, but this resulted in poor fitting to experimental data. It was necessary to use estimated diffusion coefficients of the monomeric radicals in the specific copolymer being synthesized. It was found that this value may strongly depend on the copolymer composition. The values used in this work for diffusion coefficients must be regarded as empirical estimates that work well for the limited set of conditions tested, but true values are expected to be composition dependent and must be obtained by independent experiments. The model turned out to be very sensitive to the values of the estimated diffusion coefficients.

In order to perform the fitting of unknown or uncertain parameters, it was necessary first to perform a study of the parametric sensitivity of the model. The main qualitative findings of this study can be summarized as follows:

—Both the rate of polymerization and the number of particles increase when the entry rate coefficient increases.

—Parameters that affect the phenomenon of emulsifier adsorption in particles Γ_∞ and b_s have a negligible effect on conversion–time curves. On the other hand, the CMC and the a_{em} of the surfactant exhibit an important effect on the evolution of conversion and average particle diameter.

—Diffusion coefficients of monomeric radicals affect the polymerization rate and the number of particles due to their influence on radical desorption. Increased radical desorption results in a larger number of particles and a decrease in polymerization rate due to the absence of radicals in polymer particles.

Methyl Methacrylate/Styrene System

For data at 60°C, one set of parameter values was fitted for runs 1, 5, and 10 (Figs. 1 and 2) with a monomer molar ratio of 70/30 MMA/S and another set of values for experiments 3 and 12, with a 30/70 MMA/S monomer molar ratio (Figs. 3 and 4). However, most of the parameters were kept constant for the two sets; the only ones changed were the micellar area covered by a surfactant molecule a_{em}, the surfactant CMC, and the effective diffusion coefficients. Parameter a_{em} of the surfactant, as discussed before, may depend on copolymer composition.[3,12] Diffusion coefficients are also expected to depend on copolymer composition; the higher the MMA content in the copolymer the lower the diffusion coefficients. This may point out to the same origin causing a more

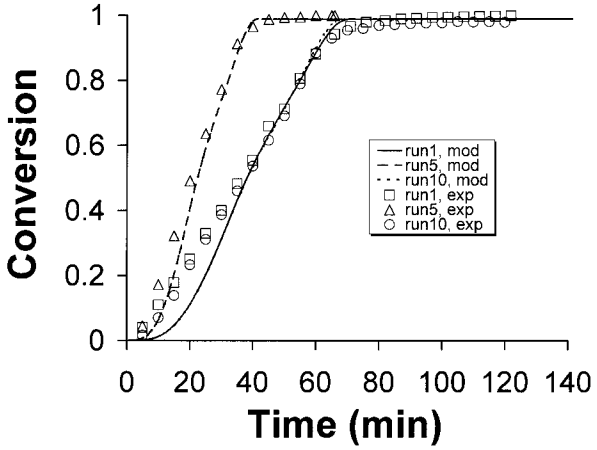

Figure 1 Model and experimental conversion–time curve for the S/MMA system, runs 1, 5, and 10.

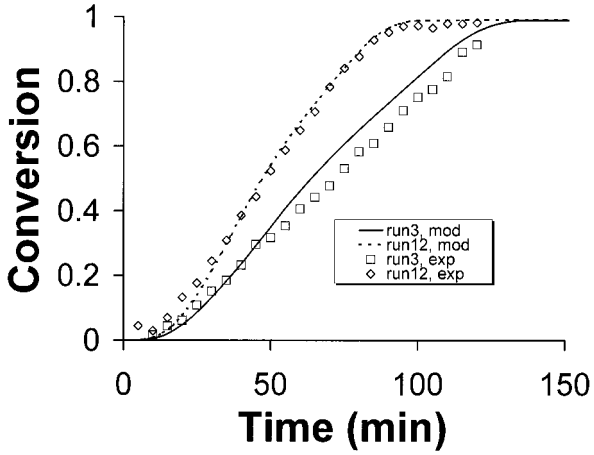

Figure 3 Model and experimental conversion–time curve for the S/MMA system, runs 3 and 12.

intense gel effect in MMA than in styrene homopolymerization (see for example ref. 42). The set of adjusted parameters is given in Tables VI and VII; the rest of the parameters is given in Appendix B.

Runs 1 and 10 have very similar histories of conversion and average particle size; they are hardly distinguishable by looking at the experimental data. Run 1 was formulated with a higher monomer to water ratio and a higher level of surfactant than run 10. These two factors affect the rate of polymerization in opposite direction: the higher monomer to water ratio the smaller the reaction rate (if concentrations of surfactant and initiator with respect to water are kept constant). On the other hand, the higher the surfactant concentration the faster the reaction rate. In this case these two effects are canceled out, yielding each other basically the same reaction rate for both. A similar situation is observed for the average particle size. The model correctly predicts the quantitative cancellation of these opposite effects. Runs 3 and 12 differ by the monomer to water ratio. At a lower ratio of monomer to water there is a larger number of particles per liter of water.

Model conversion evolution curves show reasonable quantitative agreement with experimental data. With respect to average particle size, there is still significant lack of fit between model and experiment; however, the model qualitatively captures the relationship between particle size and reaction rate; that is, the smaller the particle

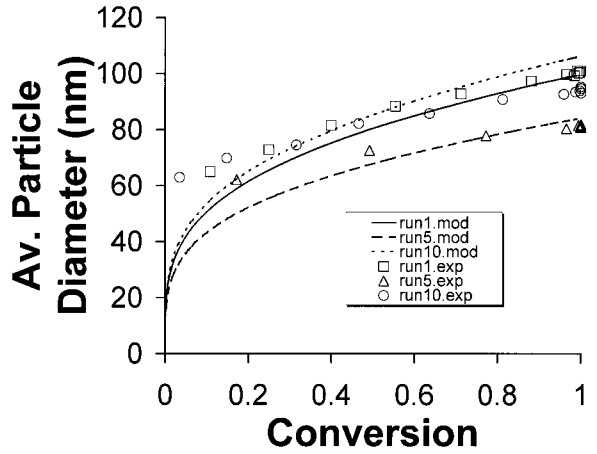

Figure 2 Model and experimental average particle diameter–conversion curve for the S/MMA system, runs 1, 5, and 10.

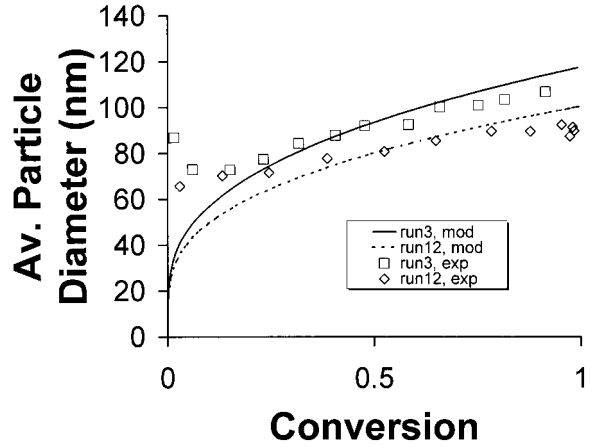

Figure 4 Model and experimental average particle diameter–conversion curve for the S/MMA system, runs 3 and 12.

Table VI Values of Parameters Fitted for Runs 1, 5, and 10 of Methacrylate/Styrene System

Parameter	Value	Units
$k_{m_m} = k_{m_p}$	8.564×10^{-7}	m/s
a_{em}	9.38×10^{-20}	m^2
CMC	8×10^{-4}	gmol/L
$D_{\text{eff},1}$	6.2×10^{-12}	m^2/s
$D_{\text{eff},2}$	4.3×10^{-15}	m^2/s
Gel effect, A_5	7.0×10^{-3}	L
Gel effect, A_7	350	L^{-1}

size the larger the number of particles and the faster the reaction rate. Lack of fit of model predictions and experimental average particle size evolution is a consequence of the complexity of the nucleation phenomena, which is still not completely understood. In the mathematical model used here nucleation phenomena is assumed to exclusively occur by the micellar mechanism. Although the trends are well predicted by this mechanism and apparently dominated by it, the experimental data suggest the presence of additional nucleation mechanisms.

Butyl Acrylate/Styrene System

Runs 1, 6, 7, and 12 were all performed at 60°C with a monomer molar ratio of 30/70 BuA/S so they are analyzed together. Values of parameters fitted are given in Table VIII. Comparison of experimental and model-predicted curves is made in Figures 5 and 6; they correspond to conversion - time and average particle size– conversion, respectively. It is noteworthy the fact that the model gives quantitative agreement with the experimental data for three of the four conversion–time curves, even when the experimental design included changes in several variables from experiment to experiment. For average particle size, the performance of the model is similar to that

Table VII Values of Parameters Changed for Fitting Runs 3 and 12 of Methyl Methacrylate/ Styrene System

Parameter	Value	Units
a_{em}	11×10^{-20}	m^2
CMC	8×10^{-3}	gmol/L
$D_{\text{eff},1}$	1.1×10^{-10}	m^2/s
$D_{\text{eff},2}$	9×10^{-14}	m^2/s

Table VIII Values of Parameters Fitted for Runs 1, 6, 7, and 12 of Butyl Acrylate/Styrene System

Parameter	Value	Units
$k_{m_m} = k_{m_p}$	3.0×10^{-6}	m/s
a_{em}	7.5×10^{-20}	m^2
CMC	6.25×10^{-4}	gmol/L
$D_{\text{eff},1}$	1.5×10^{-12}	m^2/s
$D_{\text{eff},2}$	3.55×10^{-16}	m^2/s
Gel effect, A_5	9.5×10^{-2}	L
Gel effect, A_7	200	L^{-1}

observed for the MMA/S system displaying still lack of fit between model and experiment but capturing qualitatively the relationship between particle size and reaction rate. It is important to note that particle size measurementes at low conversions (less than 20%) are not reliable. This is due to the fact that light scattering averages tend to weigh more heavily larger particles; at low conversions particles are small and the presence of a few large particles arising from latex instability may shift the measurement to larger particle sizes.

Also, model and experimental conversion–time curves for runs 5 and 13, performed at 60°C and having a monomer molar ratio 70/30 BuA/S are shown in Figure 7. Values of additional parameters fitted are given in Table IX. Notice that the only parameter values changed with respect to the values used for the 30/70 BuA/S molar ratio data are the micelle surface area covered by a surfactant molecule and the gel effect parameters

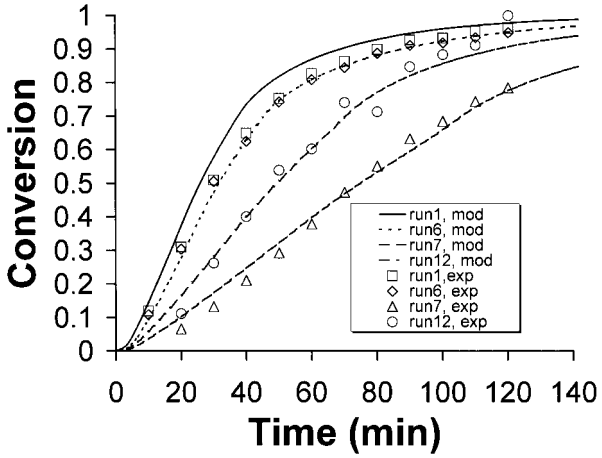

Figure 5 Model and experimental conversion–time curve for the S/BuA system, runs 1, 6, 7, and 12.

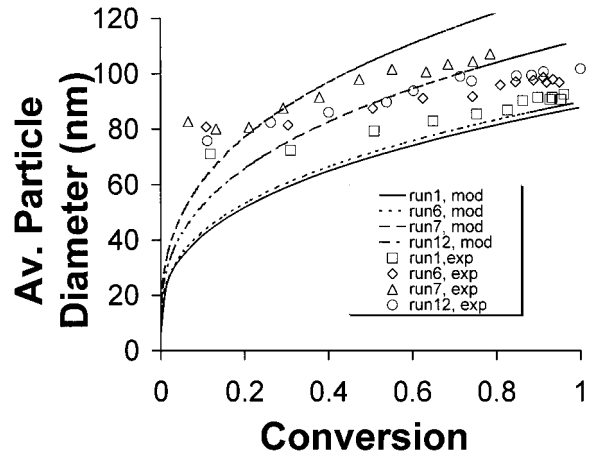

Figure 6 Model and experimental average particle diameter–conversion curve for the S/BuA system, runs 1, 6, 7, and 12.

for butyl acrylate. The change in gel effect parameters for butyl acrylate at different monomer molar ratio in the feed arises from the semiempirical nature of the gel effect model for a copolymerization system.

With respect to the particle size–conversion data for runs 5 and 13, the model underpredicts the experimental values (30% error), although the relative location of the curves (not shown) is correctly given by the model.

General trends observed for the fitted parameters are as follows:

—Parameter a_{em} of the surfactant increases with increased content of butyl acrylate

—Gel effect A_5 parameter (critical free volume for onset of glass effect) increases with increasing butyl acrylate content. This means that the onset of glass effect occurs earlier for larger contents of butyl acrylate. A reason for this behavior could be the hindered diffusion caused by increased crosslinking in presence of higher content of BA. The opposite effect is observed for parameter A_7.

Table IX Values of Parameters Changed for Fitting Runs 5 and 13 of Butyl Acrylate/Styrene System

Parameter	Value	Units
a_{em}	20×10^{-20}	m^2
Gel effect, A^5	10.5×10^{-2}	L
Gel effect, A_7	160	L^{-1}

Butadiene/Styrene System

For the purpose of analysis and fitting, experimental data for this system were split in two sets: (1) runs 1, 5, 15, and 16 with a molar ratio 30/70 (B/S) and (2) runs 2, 6, 14, 17, and 18 at a molar ratio 70/30 (B/S). Notice that all runs were performed at 70°C, except for runs 16, 17 and 18 at 80°C. For the first set model and experimental curves displayed in Figure 8 correspond to conversion evolution and in Figure 9 to average particle size–conversion; the agreement of model and experiments is good. Parameters fitted are given in Table X.

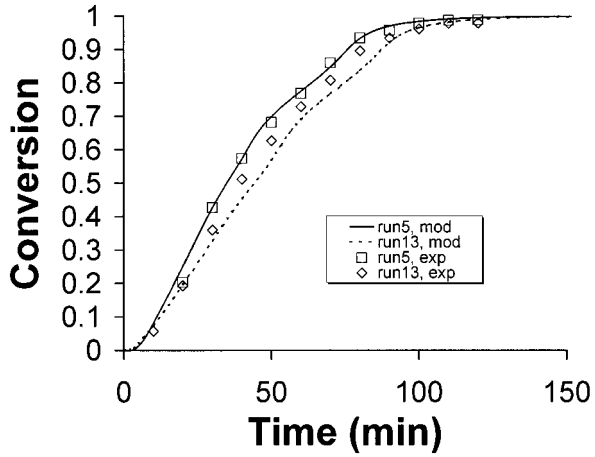

Figure 7 Model and experimental conversion–time curve for the S/BuA system, runs 5 and 13.

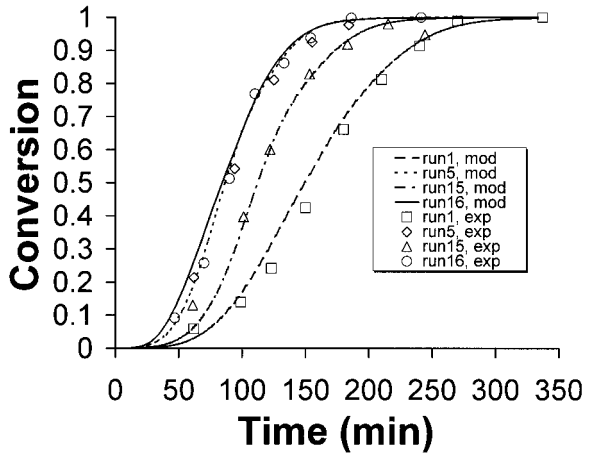

Figure 8 Model and experimental conversion–time curve for the S/B system, runs 1, 5, 15, and 16.

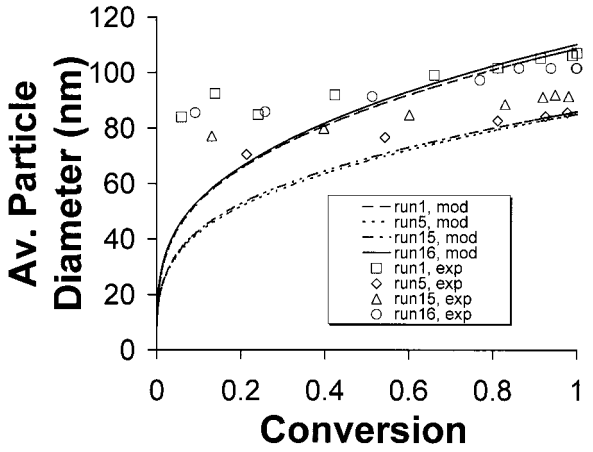

Figure 9 Model and experimental average particle diameter–conversion curve for the S/B system, runs 1, 5, 15, and 16.

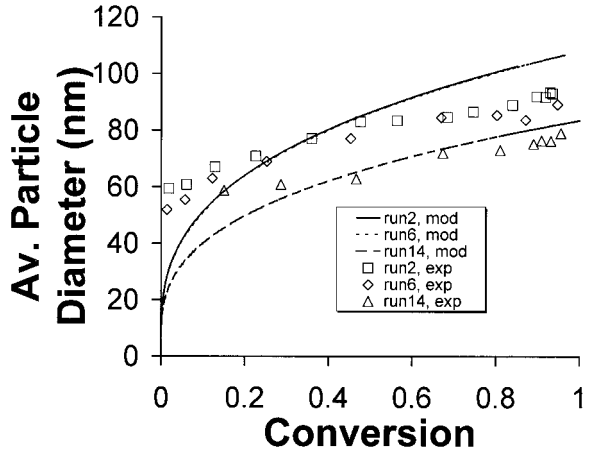

Figure 10 Model and experimental average particle diameter– conversion curve for the S/B system, runs 2, 6, and 14.

On the other hand, for the second set of experiments with a higher content of butadiene, fitting was more difficult. The effect of initiator concentration on reaction rate was overpredicted by the model and could not be fitted satisfactorily, so fitting of conversion–time curves for experiments 2, 6, and 14 is not good. The only variables changed in this subset of experiments are initiator and emulsifier concentration. In fact, between runs 2 and 6 the only variation was initiator concentration. As pointed out in the literature review section, butadiene emulsion polymerization rate shows a very weak dependence, not well understood, on initiator concentration. This unusual behavior has been attributed to a low efficiency of initiator nucleating particles.[30] Apparently, above certain critical initiator concentration, the dependence of polymerization rate on initiator concentration becomes very weak, which means that the effect is nonlinear. On the assumptions of the present model, however, it is difficult to simulate this behavior since, in order to fit a given conversion history, the model adjustable parameter is actually the product of entry rate coefficient and initiator efficiency (a low efficiency value will require a large value for the entry rate coefficient and vice versa). The comparison of model and experimental curves for average particle size evolution in runs 2, 6, and 14 is shown in Figure 10; parameters fitted are given in Table XI.

Runs 17 and 18, performed at 80°C, show the emulsifier concentration effect on polymerization kinetics. Model and experimental conversion history and particle size evolution curves are given in Figures 11 and 12, respectively. Model predictions are good except for the data of particle size at low conversions. Parameter values changed for this simulation are included in Table XI.

General trends observed for the parameters fitted are as follows:

Table X Parameter Values Fitted for Runs 1, 5, 15, and 16 of Butadiene/Styrene System

Parameter	Value	Units
$k_{m_m} = k_{m_p}$	1.3×10^{-7}	m/s
a_{em}	3×10^{-20}	m^2
CMC	1.5×10^{-3}	gmol/L
$D_{\text{eff},1}$	3×10^{-13}	m^2/s
$D_{\text{eff},2}$	3.55×10^{-16}	m^2/s
Gel effect, A_5	12.0×10^{-2}	L
Gel effect, A_7	70	L^{-1}

Table XI Values of Parameters Fitted for Runs 2, 6, 14, 17, and 18 of Butadiene/Styrene System

Parameter	Value		Units
$k_{m_m} = k_{m_p}$	2.7×10^{-7} [a]	3×10^{-7} [b]	m/s
a_{em}	6×10^{-21}		m^2
$D_{\text{eff},1}$	9×10^{-11} [a]	9×10^{-12} [b]	m^2/s
$D_{\text{eff},2}$	9×10^{-14} [a]	9×10^{-15} [b]	m^2/s
Gel effect, A_5	11×10^{-2} [a]	15×10^{-2} [b]	L
Gel effect, A_7	37[a]	25[b]	L^{-1}

[a] Values at 70°C (2, 6, and 14).
[b] Values at 80°C (17 and 18).

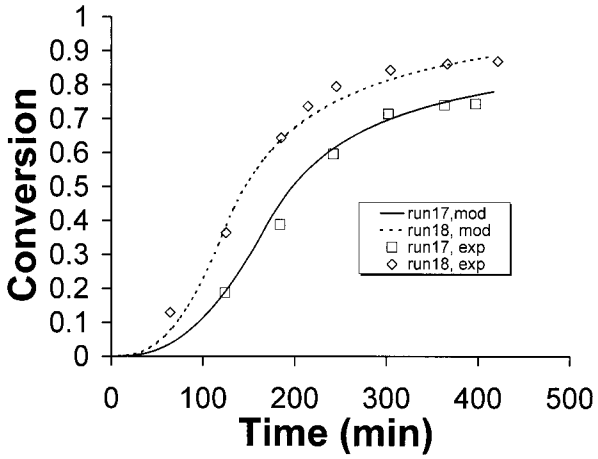

Figure 11 Model and experimental conversion–time curve for the S/B system, runs 17 and 18.

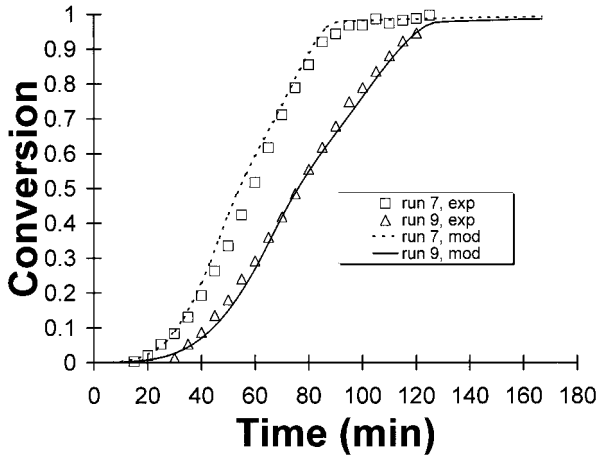

Figure 13 Model and experimental conversion–time curve for the S/AA system, runs 7 and 9.

—Entry rate coefficients tend to increase with increased content of butadiene and with increased temperature.

—Parameter a_{em} of the surfactant tends to decrease with increased content of butadiene.

—Effective difussion coefficients increase with increased content of butadiene. This effect has also been suggested by previous researchers.[30]

Acrylic Acid/Styrene System

For this system only runs 7 and 9 were analyzed and fitted. Both experiments were formulated with a monomer molar ratio of 5/95 AA/S at 60°C. Figure 13 shows the experimental data and model predictions for conversion–time curves. Figure 14 displays corresponding results for average particle diameter–conversion curves. Fitted parameters are given in Table XII. The agreement of the model with experiments is good for conversion histories and only semiquantitative for the average particle diameter evolution.

Due to the fact that the termination rate coefficient for acrylic acid has not been reported in the literature, its value was assumed the same as that for styrene polymerization. This may not introduce a large error at the 5/95 AA/S molar ratio.[43] Although other runs were performed at a 30/70 AA/S molar ratio, no attempt was made of fitting this data due to the lack of values for acrylic acid kinetic rate coefficients.

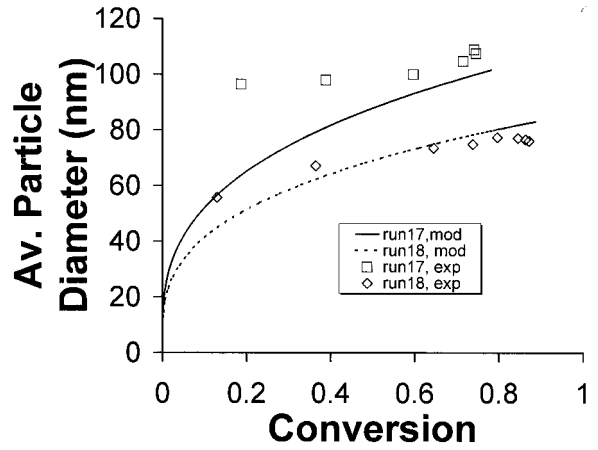

Figure 12 Model and experimental average particle diameter– conversion curve for the S/B system, runs 17 and 18.

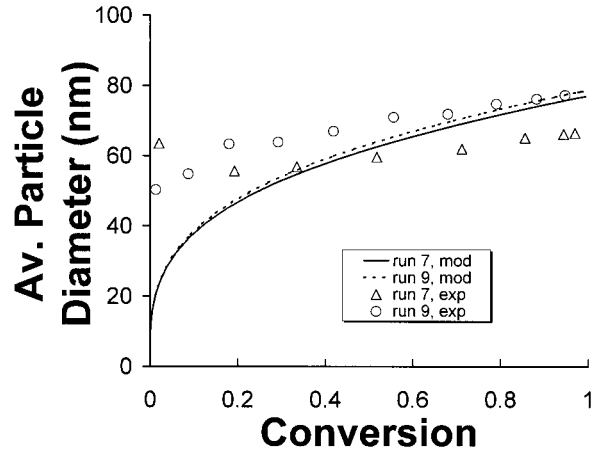

Figure 14 Model and experimental average particle diameter–conversion curve for the S/AA system, runs 7 and 9.

Table XII Values of Parameters Fitted for Runs 7 and 9 of System Acrylic Acid/Styrene

Parameter	Value	Units
k_{m1}	11.5×10^{-7}	m/s
k_{m2}	34.5×10^{-7}	m/s
a_{em}	1.5×10^{-19}	m^2
CMC	5×10^{-5}	gmol/L
$D_{\text{eff},AA}$	2.3×10^{-13}	m^2/s
$D_{\text{eff},S}$	2.3×10^{-15}	m^2/s
Gel effect, A_5	0.132	L
Gel effect, A_7	140	L^{-1}

Due to the hydrophilic character of acrylic acid a large part of it, as well as its copolymer, should be located on the latex particles surface acting, together with the surfactant, as a particle stabilizer. Therefore, fitted values for surfactant parameters should be taken as effective global values for the pair acrylic acid–surfactant.

As mentioned before, Ceska[35] found that the presence of acrylic acid increases styrene polymerization rate. This was verified in this work. Lange and Poehlein[43] found that the copolymerization with carboxylic acids can alter the rate of emulsion polymerization of styrene due to a change in the number of particles generated (through homogeneous nucleation) and an increase in the rate of radical desorption, favored by the high solubility of acrylic acid in water. The increased number of monomeric radicals in the aqueous phase tend to increase the nucleation of particles and therefore the polymerization rate. This phenomenon, however, is not completely understood so it was decided to use a single effective value for the diffusion coefficient of both monomers.

FINAL REMARKS AND CONCLUSIONS

In this paper experimental results for conversion and particle size evolution, as well as comparison with model predictions, are presented for four emulsion copolymerizations of styrene with different monomers: methyl methacrylate, butyl acrylate, butadiene, and acrylic acid. The experiments covered a wide range of conditions including variations on initiator and surfactant concentrations, water to monomer ratio, comonomer composition, and temperature. After parameter fitting of unknown and uncertain parameters of the model, this is capable of reproducing reasonably well most of the experimental curves for time evolution of conversion and of giving correct trends for evolution of average particle diameter with conversion. Micellar nucleation explains only partially the quantitative data for evolution of particle size.

An exception to the adequacy of the model in conversion–time data is given by its overprediction of the effect of initiator concentration on the rate of butadiene/styrene copolymerization with high content of butadiene (70%). However, previously published works on this system had reported on this deviation from generally accepted theories of emulsion polymerization and indicated the lack of understanding of this phenomenon. Clearly, research focused on this specific issue is needed.

It was also found that model predictions are very sensitive to the value of the diffusion coefficients of monomeric radicals in the copolymer particle, which are not readily available in the literature; therefore they had to be fitted. In general, it was found that several parameters, especially a_{em} and CMC of the surfactant, entry rate coefficients k_{mmi} and k_{mmR} and diffusion coefficients, may depend on copolymer composition.

It is important to mention that the model predicts reasonably well the evolution of copolymer composition with conversion using reactivity ratios taken from the literature. Due to space constraints, it was not possible to include plots containing comparisons of model predictions and experimental data for composition evolution; however, these plots look very much like the ones included in the first paper of the series,[36] in which a simpler model for copolymer composition evolution was used.

The results of this study indicate that, at the present level of knowledge and after some parameter fitting, a global model like the one analyzed in this work is fine for practical applications: operation, design, control, and optimization of emulsion copolymerization processes. However, considering the complexity of the system studied, the model should be taken with caution if is to be used for parameter estimation. Values of fitted parameters estimated in this work are influenced by other estimated parameters due to the global nature of the model used. In this kind of models, and even with the aid of statistical techniques and optimal experimental designs, it is not possible to estimate parameters without correlation. This points out the importance of independently mea-

suring parameters in order to get predictive modeling tools.

It should be emphasized that this is the first work in which a model for emulsion copolymerization is systematically tested, not only varying widely the experimental conditions, but also applying the model to a number of comonomer systems.

In the next paper of this series, the conclusions of this part are further tested using experimental data for additional copolymerization systems.

APPENDIX A: MATHEMATICAL MODEL

The model is in the form of a population balance equation for the particle size distribution (PSD). In the original work presented by Saldívar et al.[5] a detailed model for the molecular weight distributions (MWD) of live and dead polymer, based on population balance equations, is also included; however, given the fact that no MWD experimental data were measured in this work, the corresponding parts of the MWD model are not presented here. Simpler environmental balances for live polymer in the aqueous phase, monomer, surfactant, and other components of the emulsion system, as well as general equations for monomer partitioning complete the model. To write the population balance equations the mass of polymer was selected as internal coordinate. Some assumptions used in the model are as follows:

- The PSD is independent of the molecular weight distribution
- Monomer partitioning among the different phases (particles, aqueous phase, and monomer droplets) reaches instantaneously thermodynamic equilibrium. That is, mass transfer limitations for monomer transport between phases are neglected. Additionally, monomer concentration in particles is assumed to be independent of particle size
- The pseudo-homopolymer approximation[44] is used in both: aqueous and particle phase. This means that the copolymerization system is treated as a homopolymerization system by proper use of apparent kinetic rate coefficients.

A complex free radical kinetic scheme based on the one proposed by Arriola (see ref. 5), adapted for the emulsion case, has been implemented in the model. In Tables AI and AII, a simplified kinetic scheme is presented, in which those reactions that only affect the MWD have been omitted from the original kinetic scheme. The same symbol is used to denote each radical species and its corresponding amount or distribution function. In this way $N^{l,b}_{n,i}(m,t)$ represents growing radicals of

Table AI Kinetic Scheme for Emulsion Copolymerization. 1. Aqueous Phase

Mechanism	Kinetics
Thermal decomposition initiation	$I_w \xrightarrow{fk_d} 2R_w$
Redox initiation	$I_w + Y_1^r \xrightarrow{k_{d1}} R_w + Y_1^0 + \text{products}$
	$Y_1^0 + Y_2 \xrightarrow{k_{d2}} Y_1^r + \text{products}$
Propagation	$R_w + M_{i_w} \xrightarrow{k_{ri}} P^1_{i_w}$
	$P^l_{i_w} + M_{j_w} \xrightarrow{k^w_{pij}} P^{l+1}_{j_w}$
	$l = 1, \ldots, cr - 1$
Chain transfer to monomer	$P^l_{i_w} + M_{j_w} \xrightarrow{k^w_{tr,ij}} D^l_w + P^0_{j_w}$
	$l = 1, \ldots, cr - 1$
Chain transfer to chain transfer agent	$P^l_{i_w} + T_w \xrightarrow{k^w_{tr,iT}} D^l_w + P^0_{T_w}$
	$l = 1, \ldots, cr - 1$
Reinitiation	$P^0_{i_w} + M_{j_w} \xrightarrow{k^w_{re,ij}} P^1_{j_w}$
CTA radical reinitiation	$P^0_{T_w} + M_{j_w} \xrightarrow{k^w_{re,Tj}} P^1_{j_w}$
Termination by combination	$P^l_{i_w} + P^m_{j_w} \xrightarrow{k^w_{tc,ij}} D^{l+m}_w$
	$l = 0, \ldots, cr - 1$
Termination by disproportionation	$P^l_{i_w} + P^m_{j_w} \xrightarrow{k^w_{td,ij}} D^l_w + D^m_w$
	$l = 0, \ldots, cr - 1$
Termination by inhibition	$P^l_{i_w} + X_w \xrightarrow{k^w_{inh}} D^l_w$
	$R_w + X_w \xrightarrow{k^w_{inh}} D^0_w$
	$l = 0, \ldots, cr - 1$

Table AII Kinetic Scheme for Emulsion Copolymerization. 2. Particle Phase

Mechanism	Kinetics
Forward and reverse propagation	$N_{n,i}^{l,b} + M_{j_p} \xrightarrow{k_{p,ij}} N_{n,j}^{l+1,b}$
	$N_{n,i}^{l,b} + M_{j_p} \xleftarrow{k_{p,ij}^{r}} N_{n,j}^{l+1,b}$
Termination by combination	$N_{n,i}^{l,b} + N_{n,j}^{h,c} \xrightarrow{k_{tc,ij}} D_{n-2}^{l+h,b+c}$
Termination by disproportionation	$N_{n,i}^{l,b} + N_{n,j}^{h,c} \xrightarrow{k_{td,ij}} D_{n-2}^{l,b} + D_{n-2}^{h,c}$
Termination by inhibition	$N_{n,j}^{l,b} + X_p \xrightarrow{k_{inhp}^{j}} D_{n-1}^{l,b}$
Chain transfer to monomer	$N_{n,i}^{l,b} + M_j \xrightarrow{k_{tr,ij}} D_n^{l,b} + N_{n,j}^{0,0}$
Chain transfer to chain transfer agent (CTA)	$N_{n,j}^{l,b} + T \xrightarrow{k_{tr,T}^{j}} D_n^{l,b} + N_{n,T}^{0,0}$
Reinitiation	$N_{n,j}^{0,0} + M_i \xrightarrow{k_{re,ji}} N_{n,i}^{1,0}$
Reinitiation of CTA radical	$N_{n,T}^{0,0} + M_i \xrightarrow{k_{re,Ti}} N_{n,i}^{1,0}$

type i, length l, and branching index b, present in particles of polymer mass m having n radicals at time t. Similarly, $D_n^{l,b}(m,t)$ represents dead polymer chains of length l and branching index b, present in particles of polymer mass m having n radicals at time t. The arguments m and t have been suppressed. The subindex w is used for quantities in the aqueous phase and the subindex p is used for the particle phase. I, R, T, X, and D denote initiator, primary radicals (coming directly from the initiator), chain transfer agent, inhibitor, and dead polymer respectively. Y_1 and Y_2 are components of a redox system; the reduced and oxidized states are denoted by the superscripts r and o respectively. M_j refers to the monomer j and $P_i^{\,l}{}_w$ stands for live polymer of length l with radical type i present in the aqueous phase. The cr is the critical length for precipitation.

The following reactions, present in the original model, have been omitted here since they affect only the MWD and they were not included in the calculations for this work: backbiting (intramolecular transfer), scission after intramolecular transfer, transfer to polymer (intermolecular transfer), scission after intermolecular transfer, terminal double bond polymerization, internal double bond polymerization.

Notice that R_{wT} includes monomeric radicals ($l = 0$) that are generated by desorption.

Transfer reactions involving monomeric and CTA radicals in aqueous phase, P_{iw}^0 and P_{Tw}^0,are considered unlikely and not allowed to occur.

Particle Size Distribution

This is the core of the model and is represented by the distribution function $\mathbf{F}(m,t)dm$, which is the number of particles present per liter of water and having a polymer mass between m and $m+dm$ at time t. The resulting population balance equation (PBE) for this quantity is mathematically a partial differential equation in polymer mass and time:

$$\frac{\partial F(m,t)V_w}{\partial t} + \frac{\partial V_w F(m,t)\dfrac{dm}{dt}}{\partial m} = \frac{F^f w_w^f Q^f}{\rho_w} - \frac{F w_w Q}{\rho_w} \tag{2}$$

where V_w is the volume of water, Q is the mass flow rate, w_w is the water mass fraction, ρ_w is the water density, and the superindex f refers to the feed. The boundary condition F_B for this equation is

$$V_w F(m,t)\left.\frac{dm}{dt}\right|_{m_m^+} = F_B$$

$$= V_{aq}N_A\left(\sum_{i=1}^{c} a_m k_{m_{mi}} M[P_i]_w + a_m k_{m_{mR}} M[R]_w\right) \tag{3}$$

and the initial condition:

$$F(m, t=0) = F_0(m) \tag{4}$$

where V_{aq} is the aqueous phase volume, a_m is the surface area of a micelle, M is the micelle concentration, k_{mmi} and k_{mmR} are the entry rate coefficients for type i radicals with aqueous phase concentration $[P_i]_w$ and for primary radicals with aqueous phase concentration $[R]_w$, respectively. Only micellar nucleation has been included in

this application of the model, canceling out the homogeneous nucleation contribution.

Desorption Coefficient of Radicals in Particles

The value of the pseudo-homogeneous desorption coefficient for radicals from particles is given by the mixing rule:

$$\bar{d} = \sum_{i=1}^{c} de_i \tag{5}$$

where de_i are desorption coefficients for monomeric radicals of type i, given (for no chain transfer agent present) by

$$de_i = g_i \Psi_i \quad i = 1, \ldots, c, T \tag{6}$$

Where g_i is the type i radicals generation frequency in a particle and Ψ_i is the probability that a monomeric radical of type i will desorb before it undergoes chemical reaction. This probability is expressed as

$$\Psi_i = \frac{K_{0i}}{K_{0i} + \sum_{j=1}^{c} k_{p,ij}[M_j]_p} \quad i = 1, \ldots, c, T \tag{7}$$

$$K_{0i} = \frac{12}{d_p^2} \frac{D_{wi} D_{pi}}{m_{di} D_{pi} + 2D_{wi}} \tag{8}$$

where $k_{p,ij}$ is the propagation rate coefficient of a type i radical with a type j monomer; and $[M_j]_p$ is the monomer j concentration in particles; d_p is the particle diameter; D_{wi} and D_{pi} are the diffusion coefficients of type i monomeric radicals in aqueous phase and in particles, respectively; and m_{di} is a partition coefficient between particle and aqueous phase for monomer.

Average Number of Radicals in Particles

It is assumed that the average number of radicals in particles is a function of the particle polymer mass and is given by an algebraic equation in terms of Bessel functions from the classical Stockmayer–O′Toole[45] solution of the Smith–Ewart recurrence equation.

Balances for Species

Simpler environmental balances for live polymer in the aqueous phase, monomer, surfactant, and other components of the emulsion system complete the model. Monomer and polymer balances for c components are represented by a 2c system of ordinary differential equations (ODEs). The radical type distribution is represented by one c-dimension algebraic linear system for each one of the phases: particles and aqueous phase.The mass balance for radicals in the aqueous phase in quasi-steady state yields one nonlinear algebraic equation for the amount of total radicals in the aqueous phase.

Monomer Partitioning. Partition coefficients.

The partition coefficients are given by the following expressions:

$$K_{dwi} = \frac{[M_i]_d^m}{[M_i]_w^m} \tag{9}$$

$$K_{pwi} = \frac{[M_i]_p^m}{[M_i]_w^m} \tag{10}$$

where K_{dwi} and K_{pwi} are the partition coefficients between droplets-water and particles-water, respectively, for monomer i, $[M_i]_d^m$, $[M_i]_w^m$, and $[M_i]_p^m$ are the mass concentrations of monomer i in monomer droplets, aqueous phase and particles, respectively. Maximum polymer swelling with monomer is defined as

$$\frac{V_P \sum_{j=1}^{c} [M_i]_p^m}{P} = A \tag{11}$$

where V_p is the volume of particles, P is the total amount of polymer on a mass basis, and A is an empirical constant.

Surfactant Partitioning

It is assumed that the surfactant adsorbed in the particles can be represented by a Langmuir type isotherm:

$$S_a = \frac{S_P \Gamma_\infty b_s S_F / V_{aq}}{1 + b_s S_F / V_{aq}} \tag{12}$$

where S_p is the total surface area of particles, S_F is the free surfactant in the aqueous phase, Γ_∞ and b_s are emprirical parameters. The value of S_F determines the surfactant concentration in the

aqueous phase $[S]_w$ and therefore the presence of micelles through the following equation:

$$M' = \frac{([S]_w - [S]_w^{cmc})N_A a_{em}}{a_m} \quad (13)$$

$$M = M'H(M') \quad (14)$$

where $[S]_w^{cmc}$ is the CMC of the surfactant, a_{em} is the area of the micelle covered by a surfactant molecule, and H is the Heaviside function.

APPENDIX B: ADDITIONAL PARAMETERS

See Tables AIII–AVI.

Table AIII Parameters Taken from the Literature or Estimated *a priori* for the Methyl Methacrylate/Styrene System

Symbol	Parameter (units)	Value [Ref.]	Conditions
ρ_s	Styrene density (kg/L)	0.909	20°C
ρ_M	Methyl methacrylate density (kg/L)	0.936	20°C
E_{PS}	Styrene propagation activation energy (kJ/mol)	26 [46]	
A_{PS}	Arrhenius styrene propagation constant (cm^3/mol/s)	0.45×10^{10} [46]	
E_{PM}	Methyl methacrylate propagation activation energy (kJ/mol)	26.4 [46]	
A_{PM}	Arrhenius methyl methacrylate propagation constant (cm^3/mol/s)	0.087×10^{10} [46]	
r_s	Styrene reactivity ratio	0.468 [12]	50°C
		0.52 [46]	60°C
		0.59 [46]	131°C
r_M	Methyl methacrylate reactivity ratio	0.461 [12]	50°C
		0.46 [46]	60°C
		0.54 [46]	131°C
E_{TS}	Styrene termination activation energy (kJ/mol)	8.0 [46]	
A_{TS}	Arrhenius styrene termination constant (cm^3/mol/s)	0.058×10^{12} [46]	
E_{TM}	Methyl methacrylate termination activation energy (kJ/mol)	11.9 [46]	
A_{TM}	Arrhenius methyl methacrylate termination constant (cm^3/mol/s)	0.11×10^{12} [46]	
Γ_∞	Surfactant adsorption isotherm parameter (mol/m^2)	3.5×10^{-6} [5]	
b_s	Surfactant adsorption isotherm parameter (L/mol)	2000 [5]	
A_6	Gel effect parameter	1.367×10^{-5}	

Table AIV Parameters Taken from the Literature or Estimated *a priori* for the Butadiene/Styrene System

Symbol	Parameter (units)	Value [Ref.]	Conditions
ρ_s	Styrene density (kg/L)	0.908	20°C
ρ_B	Butadiene density (kg/L)	0.521	20°C
E_{PS}	Styrene propagation activation energy (kJ/mol)	26 [46]	
A_{PS}	Arrhenius styrene propagation constant (cm^3/mol/s)	0.45×10^{10} [46]	
E_{PB}	Butadiene propagation activation energy (kJ/mol)	35.7 [32]	
A_{PB}	Arrhenius butadiene propagation constant (cm^3/mol/s)	11.2×10^{10} [32]	
r_s	Styrene reactivity ratio	0.58 [46]	50°C
r_B	Butadiene reactivity ratio	1.4 [46]	50°C
E_{TS}	Styrene termination activation energy (kJ/mol)	8.0 [46]	
A_{TS}	Arrhenius styrene termination constant (cm^3/mol/s)	0.058×10^{12} [46]	
E_{TB}	Butadiene termination activation energy (kJ/mol)	8.0 [46]	Estimated
A_{TB}	Arrhenius butadiene termination constant (cm^3/mol/s)	0.058×10^{12} [46]	Estimated
Γ_∞	Surfactant adsorption isotherm parameter (mol/m^2)	3.5×10^{-6} [5]	
b_s	Surfactant adsorption isotherm parameter (L/mol)	2000 [5]	
A_6	Gel effect parameter	$2.2 \times 10^{-4}/1.7 \times 10^{-2}$ (70°C) 2.3×10^{-2} (80°C) (Table 10/11)	

Table AV Parameters Taken from the Literature or Estimated a priori for the Butyl Acrylate/Styrene System

Symbol	Parameter (units)	Value [Ref.]	Conditions
ρ_s	Styrene density (kg/L)	0.909	20°C
ρ_{AB}	Butyl acrylate density (kg/L)	0.894	20°C
E_{PS}	Styrene propagation activation energy (kJ/mol)	26 [46]	
A_{PS}	Arrhenius styrene propagation constant (cm^3/mol/s)	0.45×10^{10} [46]	
k_{PAB}	Butyl acrylate propagation constant (cm^3/mol/s)	2.47×10^5 [47]	60°C
r_s	Styrene reactivity ratio	0.80 [46]	60°C
r_{AB}	Butyl acrylate reactivity ratio	0.15 [46]	60°C
E_{TS}	Styrene termination activation energy (kJ/mol)	8.0 [46]	
A_{TS}	Arrhenius styrene termination constant (cm^3/mol/s)	0.058×10^{12} [46]	
k_{TAB}	Butyl acrylate termination constant (cm^3/mol/s)	5.6×10^8 [47]	60°C
Γ_∞	Surfactant adsorption isotherm parameter (mol/m^2)	3.5×10^{-6} [5]	
b_s	Surfactant adsorption isotherm parameter (L/mol)	2000 [5]	
A_6	Gel effect parameter	5.60×10^{-9}/ 5.06×10^{-9} (Table 8/9)	

Table AVI Parameters Taken from the Literature or Estimated a priori for the Acrylic Acid/Styrene System

Symbol	Parameter (units)	Value [Ref.]	Conditions
ρ_s	Styrene density (kg/L)	0.909	20°C
ρ_{AA}	Acrylic acid density (kg/L)	1.051	20°C
E_{PS}	Styrene propagation activation energy (kJ/mol)	26 [46]	
A_{PS}	Arrhenius styrene propagation constant (cm^3/mol/s)	0.45×10^{10} [46]	
k_{PAA}	Acrylic acid propagation constant (cm^3/mol/s)	15×10^5 [43]	70°C, pH 2.8 to 3
r_s	Styrene reactivity ratio	0.15 [46]	60°C
r_{AA}	Acrylic acid reactivity ratio	0.25 [46]	60°C
E_{TS}	Styrene termination activation energy (kJ/mol)	8.0 [46]	
A_{TS}	Arrhenius styrene termination constant (cm^3/mol/s)	0.058×10^{12} [46]	
E_{TAA}	Acrylic acid termination activation energy (kJ/mol)	8.0 [46]	Estimated
E_{TAA}	Arrhenius acrylic acid termination constant (cm^3/mol/s)	0.058×10^{12} [46]	Estimated
Γ_∞	Surfactant adsorption isotherm parameter (mol/m^2)	3.5×10^{-6} [5]	
b_s	Surfactant adsorption isotherm parameter (L/mol)	2000 [5]	
A_6	Gel effect parameter	9.7×10^{-9}	

The authors wish to thank Prof. W. Harmon Ray and the sponsors of the University of Wisconsin Polymerization Reaction Engineering Laboratory (UWPREL), for permission using experimental data obtained in their laboratory, use of the POLYRED software package, and generous financial support and hospitality during the project. The authors are also grateful for valuable comments and discussions with Prof. Ray. O. Araujo wishes to thank CNPq, Brasil for financial support. E. Saldívar also thanks CID-GIRSA for financial support.

REFERENCES

1. García-Rubio, L. H.; Lord, M. G.; MacGregor, J. F.; Hamielec, A. E. Polymer 1985, 26, 2001–2013.
2. Rawlings, J. B.; Ray, W. H. Polym Eng Sci 1988, 28, 257–274.
3. van Herk, A. M.; German, A. L. Macromol Theory Simul 1998, 7, 557–565.
4. Araujo, O. Ph.D. Thesis (in Portuguese), Polytechnic School, University of Sao Paulo, Brazil, 1997.
5. Saldívar, E.; Dafniotis, P.; Ray, W. H. J Macromol Sci-Rev Macromol Chem Phys 1998, C38(2), 205–323.
6. Ballard, M. J.; Napper, D. H.; Gilbert, R. G. J Polym Sci Polym Chem Ed 1981, 19, 939–954.
7. Goldwasser, J. M.; Rudin, A. J Polym Sci Polym Chem. 1982, 20, 1993.
8. Nomura, M.; Yamamoto, K.; Horie, I. M.; Fujita, K. J Appl Polym Sci 1982, 27, 2483–250l.
9. Chen, S.; Wu, K. J Polym Sci Part A: Polym Chem Ed 1988, 26, 1487–1506.

10. Nomura, M. Horie, I.; Kubo, M.; Fujita, K. J Appl Polym Sci 1990, 37, 1029.
11. Nomura, M.; Takahashi, K.; Fujita, K. Makromol Chem Macromol Symp 1990, 35/36, 13.
12. Forcada, J.; Asua, J. M. J Polym Sci Part A Polym Chem 1990, 28, 987.
13. Forcada, J.; Asua, J. M. J Polym Sci Part A Polym Chem Ed 1991, 29, 1231–1242.
14. Noel, L. F. J.; Van Zon, J. M. A. M.; Maxwell, I. A.; German, A. L. J Polym Sci Part A: Polym Chem 1994, 32, 1009–1026.
15. Cruz, M. A.; Palacios, J.; Rejón, G.; F., Ruiz, L. M.; Ríos, L. Makromol Chem Suppl 1985, 10/11, 87.
16. Cruz-Rivera, M. A.; Ríos-Guerrero, L.; Monnet, C.; Schlund, B.; Guillot, J.; Pichot, C. Polymer 1989, 30, 1872–1882.
17. Guillot, J. Makromol Chem Macromol Symp 1990, 35/36, 269–289.
18. Canegallo, S.; Canu, P.; Morbidelli, M.; Storti, G. J Appl Polym Sci 1994, 54, 1919.
19. Guggliotta, L. M.; Brandolini, M. C.; Vega, J. R.; Iturralde, E. O.; Azum, J. L.; Meira, G. R. Polym React Eng 1995, 3(3), 201–233.
20. López de Arbina, L.; Barandiaran, M. J.; Gugliotta, L. M.; Asua, J. M. Polymer 1997, 38, 143.
21. Mitchel, J. M.; Williams, H. L. Can J Res 1948, 27, 35–46.
22. Carr, C. W.; Kolthoff, I. M.; Meehan, E. J.; Stenberg, R. J. J Polym Sci 1950, 5(2), 191.
23. Carr, C. W.; Kolthoff, I. M.; Meehan, E. J.; Stenberg, R. J. J Polym Sci 1950, 5(2), 201.
24. Burnett, G. M.; Cameron, G. G.; Thorat, P. L. J Polym Sci A-1 1970, 8, 3435.
25. Burnett, G. M.; Cameron, G. G.; Thorat, P. L. J Polym Sci A-1 1970, 8, 3443.
26. Burnett, G. M.; Cameron, G. G.; Thorat, P. L. J Polym Sci A-1 1970, 8, 3455.
27. Hamielec, A. E.; Macgregor, J. F.; Penlidis, A. In Reichter, K. H., Geiseler, W., Eds.; Polymer Reaction Engineering; Hanser: Munich, 1983; pp 21–71.
28. Broadhead, T. O.; Hamielec, A. E.; Macgregor, J. F. Makromol Chem Suppl 1985, 10/11, 105–128.,
29. Sayer, C.; Lima, E. L.; Pinto, J. C. Chem Eng Sci 1997, 52(3), 341–356.
30. Weerts, P. A.; van der Loss, J. L. M; German, A. L. Makromol Chem 1989, 190, 777–788.
31. Bachmann, R.; Kruse, C.; Oppenheimer-Stix, C.; Reif, L.; Muller, H. G. DECHEMA Monographs; Wiley—VCH, 1998; Vol 134, pp 449–457.
32. Bachmann, R.; Pallaske, U.; Schmidt, A.; Muller, H. G. DECHEMA Monographs; VCH, 1995; Vol 131, pp 65–74.
33. Tobita, H.; Hamielec, A. E. Crosslinking Kinetics in Free-Radical Copolymerization, Polym. Reac. Eng; Reichert, K. H.; Geiseler, W. Eds.; VCH: Berlin, 1989; p 43.
34. Charmot, D.; Guillot, J. Polymer 1992, 33, 2, 353.
35. Ceska, G. W. J. Appl Polym Sci 1974, 18, 427.
36. Araujo, O.; Giudici, R.; Saldívar, E.; Ray, W. H. J Appl Polym Sci 1999, in press.
37. Saldívar, E.; Ray, W. H. Ind Eng Chem Res 1997, 3(4), 1322–1336.
38. Petzold, L. R. DASSL: A Differential—Algebraic System Solver, Internal Report, Sandia National Laboratories, 1985.
39. Morbidelli, M.; Storti, G.; Carrá, S. J Appl Polym Sci 1983, 28, 901–919.
40. Maxwell, I. A.; Morrison, B. R.; Napper, D. H.; Gilbert, R. G. Macromolecules 1991, 24, 1629–1640.
41. Schmidt, A. D.; Ray, W. H.Chem Eng Sci 1981, 36, 1401–1410.
42. Tulig, T. J.; Tirrell, M. Macromolecules 1981, 14, 1501–1511.
43. Lange, D. M.; Poehlein, G. W. Polym Reac Eng 1992–1993, 1(1), 41–73.
44. Storti, G.; Carrá, S.; Morbidelli, M.; Vita, G. J Polym Sci Polym Chem Ed 1989, 37, 2443–2467.
45. O'Toole, J. T. J Appl Polym Sci 1965, 9, 1291–1297.
46. Brandrup, J.; Immergut, E. H. Polymer Handbook, 3rd Ed.; Wiley Interscience: New York, 1989.
47. Gugliotta, L. M.; Arzamendi, G.; Asua, J. M. J Appl Polym Sci 1995, 55, 1017.